Interlayer Magnetoresistance of Quasi-One-Dimensional Layered Organic Conductors

W. Kang,[1,2,*] T. Osada,[2] Y. J. Jo,[1] and Haeyong Kang[1]

[1]*Department of Physics, Ewha Womans University, Seoul 120-750, Korea*

[2]*Institute for Solid State Physics, University of Tokyo, Kashiwa, Chiba 277-8581, Japan*

(Received 5 September 2006; published 5 July 2007)

We studied the interlayer magnetoresistance of the representative quasi-one-dimensional (Q1D) layered organic conductor, $(TMTSF)_2PF_6$, over the full range of magnetic field orientations in three dimensions, and constructed a stereographic conductivity plot. Our results show that the previously reported angular-dependent magnetoresistance phenomena in Q1D conductors are closely related to one another in intermediate field orientations. Based on a comparison with theories, we can conclude that the Lebed resonance is the only fundamental effect and that other effects result from the modulation of the Lebed resonance amplitude. Most of the observed phenomena can be explained within the framework of the conventional Fermi liquid; however, the anomalous enhancement of the interlayer conductivity under a field parallel to the conducting planes suggests the existence of a new electron state.

DOI: 10.1103/PhysRevLett.99.017002 PACS numbers: 74.70.Kn, 71.18.+y, 72.15.Gd

Low-dimensional electrons display various characteristics that cannot be explained by the Landau Fermi liquid theory. For example, the dramatic oscillatory and resonance phenomena exhibited by layered organic conductors as a function of magnetic field orientation [1–3] are often cited as evidence of non-Fermi liquid behavior. Variations in physical quantities with changing the azimuthal angle reflect in-plane anisotropy of the system. Hence layered electron systems with strong in-plane anisotropy, such as quasi-one-dimensional (Q1D) conductors, are expected to show marked azimuthal angle dependence.

In fact, various types of angular effects have been observed in Q1D organic conductors. Lebed magic angle resonances have been observed under rotation of the field in the plane perpendicular to the 1D axis (a axis) [4–7], and Danner-Kang-Chaikin (DKC) oscillations have been found under rotation of the field in the plane defined by the 1D axis and the normal of the layers [8,9]. In addition, the third angular effect (TAE) was observed in the case of field rotation in the layer plane [10,11]. (See the inset of Fig. 1 for the principal axes.) In a detailed study of the interlayer resistance around the 1D axis, Lee and Naughton showed that a complicated pattern develops if a small component of the magnetic field is added perpendicular to the main crystalline plane. They found that some of the peaks in this pattern are closely related to the Lebed resonances and suggested that the semiclassical Boltzmann transport equation can be used to simulate all three oscillatory effects [12,13].

No less than a dozen theoretical models have been proposed to explain the aforementioned phenomena [2,14–28]. Some recently developed models can describe the interlayer resistance for arbitrary magnetic field directions [18–20,25]. However, a lack of three-dimensional experimental data makes it impossible to test these models. One example of the long-standing puzzles is the fact that Lebed resonance has been observed experimentally in the bc plane yet some of the above theories predict its absence.

Given the fragmented state of previous experimental and theoretical work in this area, a stereographic study is urgently needed that examines the overall behavior of a single sample type under constant environmental conditions and that seeks to elucidate the genuine nature of the interlayer electron transport in that system. The tetramethyltetraselenafulvalene (TMTSF) family of Q1D organic conductors (Bechgaard salts) is ideal for this purpose.

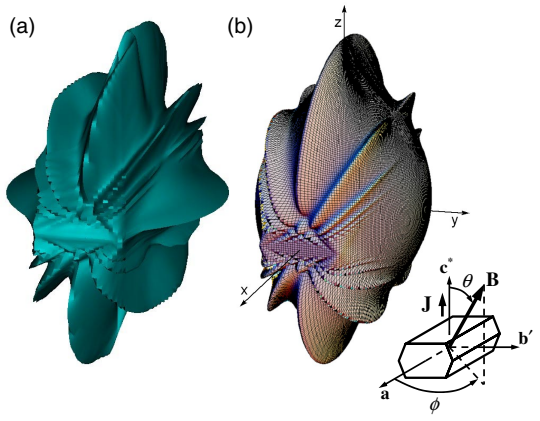

FIG. 1 (color online). Stereographic presentation of interlayer conductivity. (a) Three-dimensional presentation of the experimentally measured interlayer conductivity, $\sigma_{zz}(\theta, \phi)$, of $(TMTSF)_2PF_6$. The origin of the plot is set as $\sigma_{zz}(\theta, \phi) = 1\ \Omega^{-1}\,\mathrm{cm}^{-1}$ and the conductivity is plotted on a logarithmic scale so that the radial distance from the origin is proportional to $\log\sigma_{zz}(\theta, \phi)$. (b) Stereographic presentation of analytically calculated $\log\sigma_{zz}(\theta, \phi)$ on a relative scale, based on Eq. (2) in the text. $t_a{:}t_b{:}t_c = 1{:}0.1{:}0.003$, $a{:}b{:}c = 1{:}2{:}3.7$, $\nu_F(beB/\hbar)\tau = 20$, and the orthorhombic symmetry is assumed for simplicity. The diagram in the bottom right corner shows a sample of $(TMTSF)_2PF_6$ with the definitions of the angles used in the text.

Metallic $(TMTSF)_2PF_6$ is especially well suited because it is free from anion ordering [6]. However, essentially similar results could be obtained with $(TMTSF)_2ClO_4$ or $(TMTSF)_2ReO_4$.

We measured the interlayer magnetoresistance of a pressurized $(TMTSF)_2PF_6$ sample with a two-axis rotator and constructed a three-dimensional picture for the interlayer conductivity under a magnetic field. Our results clearly show that all of the previously reported experimental results are special cases of a more general three-dimensional phenomenon, as suggested by some theories [16–20]. Furthermore, our results confirm that the Lebed magic angle resonance is the only fundamental effect and that other effects are the result of modulation of the Lebed resonance amplitude. Most of the observed phenomena can be explained either within the conventional Fermi liquid framework [21] or (in)coherent interplane single particle tunneling [16–20]; however, the interlayer conductivity shows anomalous enhancement when the field is parallel to the conducting planes.

A special two-axis rotator probe was used to rotate a BeCu pressure cell (14 mm in diameter and 20 mm long) three dimensionally in a standard superconductor solenoid. Electrical contacts with 20 μm annealed gold wires were assured with carbon paste. An ac current of 10 μA was applied along the interlayer direction (i.e., along the c^* axis) and the voltage across the sample was measured using a lock-in amplifier. Daphne 7373 oil was used as the pressure transmitting medium. The pressure at low temperature was 8.4 kbar, as estimated from the superconductivity transition temperature of high-purity (99.999%) tin embedded near the samples. Temperature was maintained at 1.5 K by pumping the helium bath. $(TMTSF)_2PF_6$ is not superconducting under these conditions. All presented data were measured at a fixed magnetic field of 8 T.

The novel centerpiece of our results is the three-dimensional picture of interlayer conductivity (or resistivity) as a function of field orientation constructed from the measured $R_{zz}(\theta, \phi)$ at many successive fixed ϕ values in fine intervals. The three-dimensional image of $\sigma_{zz}(\theta, \phi)$ seen from $\theta = 80°$ and $\phi = 20°$ direction shown in Fig. 1(a) provides a never before seen perspective on interlayer electron transport in layered conductors with strong in-plane anisotropy. It not only shows all of the previously reported angular effects, but also the subtle relationship among them and how they evolve in the intermediate angular regions.

In Fig. 1(a), we can clearly see that the most fundamental angular-dependent structures are sharp ridges parallel to the $a(x)$ axis, corresponding to the Lebed resonances where the B_y and B_z components satisfy the following generalized magic angle condition [12,18]:

$$\frac{B_y}{B_z} = \tan\theta \sin\phi = \frac{p}{q} \frac{b \sin\gamma}{c \sin\beta \sin\alpha^*} - \cot\alpha^* \qquad (1)$$

regardless of B_x. Here, b, c, β, and γ are lattice parameters, α^* is defined by $\cos\alpha^* = (\cos\gamma \cos\beta - \cos\alpha)/\sin\beta \sin\gamma$, and p and q are small integers ($N = p/q$, $q = 1$). A particularly noteworthy feature of the present data is that the Lebed resonances become even larger when the B_x component is finite. The Lebed resonance is extremely robust and almost omnipresent on the 4π rotation, with its amplitude oscillating as a function of B_x. However, at $B_x = 0$ (i.e., on the yz plane), most of the Lebed resonances with indices $|N| > 1$ have amplitudes that are almost zero. For example, it is clear from both Figs. 1(a) and 2(a) that the $N = \pm 2$ resonances almost vanish on approaching the yz plane. The regions where the resonances vanish are slightly out of the yz plane because the crystal has a triclinic lattice. This observation shows that, contrary to the widely held belief, that the Lebed resonance dips vanish when the field is parallel to the yz plane.

A complex pattern develops as the magnetic field direction approaches the 1D axis (x axis). It is in this region that the DKC oscillations and the TAE have been observed during the zx- and xy-plane rotations [8–11]. The detailed scan of the magnetic field in this area shows surprisingly well-developed patterns comprised of regular oscillations of $R_{zz}(\theta, \phi)$ in both the θ and ϕ directions. In Fig. 3(a), converging Lebed resonances appear as radiating bright lines, and DKC oscillations and the TAE are seen on the $\phi = 0$ and $\theta = 90°$ lines, respectively. This figure clearly shows that these three representative angular effects develop simultaneously and interfere with one another, particularly in the quite broad rhombic area around the x axis with $|\theta - 90°| \leq 15°$ and $|\phi| \leq 20°$. The present data therefore establish for the first time that these angular effects are closely connected with one another rather than being independent. The existence of a well-defined rhombic area of complex patterns also excludes the argument that the DKC oscillations are easily destroyed by the presence of the magnetic field component along the b direction, as well as the argument that Lebed magic angle effects cannot coexist with DKC oscillations [9]. A similar conclusion was drawn previously by Lee and Naughton [13]. At the largest ϕ where the pattern disappears, B_y is as large as 2 T, which is 10 times larger than the estimated threshold. Moreover, the present data establish that oscillations in Ref. [12] are not an independent phenomenon; rather, as can be seen in Fig. 3(a), they simply correspond to an oscillatory pattern along lines of constant θ near 90°.

As mentioned above, the present stereographic data have revealed close connections among the various angular effects in interlayer magnetotransport, and therefore suggest that for a theory to be of value, it must be able to explain these effects as a whole. Several analytic expressions have been developed that could potentially meet this requirement [16–18,20].

In the semiclassical model, the angular effects are explained as Fermi surface topological effects, making the existence of well-defined Fermi sheets essential. This model considers the semiclassical electron orbital motion on Fermi sheets and sums up all of their contributions [21]. The interlayer conductivity is calculated using the Boltzmann equation with a constant relaxation time. It can be shown, however, that angular effects can appear in the absence of well-defined Fermi sheets. In the tunneling model, only the lowest order contribution of interlayer coupling to the conductivity is considered, that is, the contribution from single tunneling between adjacent layers. This model was originally proposed by McKenzie *et al.* in order to show that angular effects can occur even in systems with incoherent interlayer coupling, where in-plane electron scattering is much more prevalent than interlayer tunneling [16]. At low magnetic fields, the contribution to the conductivity of single tunneling is given by the same analytic formula as for the semiclassical model. Therefore, a single tunneling process between adjacent layers can also account for the Lebed resonance and its modulatory effects; coherent electron motion on the Fermi surface is not always required.

For example, under the approximation of small interlayer coupling, t_c, in orthogonal crystals, the following analytic expression describes the interlayer conductivity [16,18,20–22]:

$$\sigma_{zz} = N(E_F)\left(\frac{et_c c}{\hbar}\right)^2 \sum_{\nu=-\infty}^{\infty} \frac{2\tau J_\nu\left(\frac{2t_b c}{\hbar v_F}\frac{B_x}{B_z}\right)^2}{1 + \nu_F^2\left(\nu\frac{beB_z}{\hbar} - \frac{ceB_y}{\hbar}\right)^2\tau^2}. \quad (2)$$

Here, v_F is the Fermi velocity along the 1D axis, and t_b and t_c are interchain transfer integrals along the y and z axes, respectively. $N(E_F) = 4/(2\pi bc\hbar v_F)$ is the density of states at the Fermi level. Interestingly, essentially identical expressions have been obtained by various authors using various hypotheses [17,18,20,22]. The stereographic plot of Eq. (2), given in Fig. 1(b), well reproduces the observed angular-dependent features in Fig. 1(a). The ridge structures correspond to the Lebed resonances. The amplitude of the νth Lebed resonance is modulated by the νth Bessel function $J_\nu(z)$ when the field is tilted with respect to the x axis. This modulation gives the DKC oscillations of each Lebed resonance. The largest peaks of the DKC oscillations converge to the TAE resonant structures in the xy plane [Fig. 3(b)]. Therefore, the Lebed resonance is the only fundamental angular effect, and the other effects result from its amplitude modulation.

Another remarkable and important result of the present study concerns the observation of enhanced interlayer conductivity when the magnetic field is parallel to the conducting layers [29]. This phenomenon manifests as an anomalous resistance dip when the magnetic field is in an in-plane direction [$|\theta| = \pm 90°$ in Fig. 2(a)]. The question of why the interlayer resistance shows a local minimum at the in-plane field orientation, where the Lorentz force works most effectively, has puzzled researchers for some time [13]. In the stereographic plot in Fig. 1(a), this in-plane anomaly appears as a brimlike feature around the xy plane. Surprisingly, the amplitude of the in-plane anomaly is almost independent of the in-plane field orientation

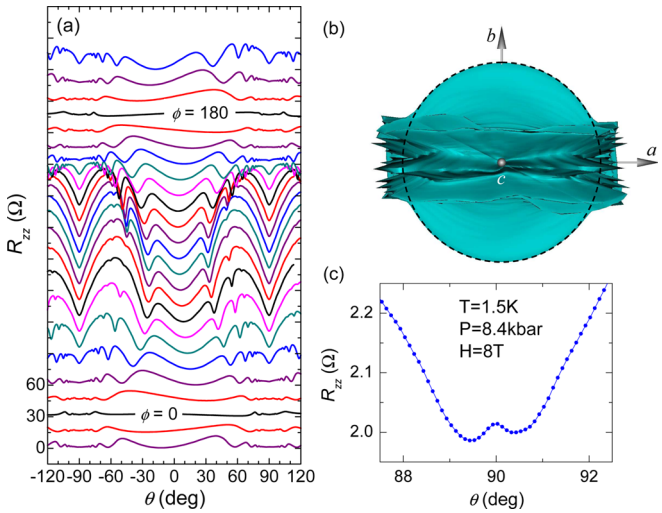

FIG. 2 (color online). (a) Typical measured resistance $R_{zz}(\theta, \phi)$ data that are used to construct the stereographic image in Fig. 1(a). The θ dependence of R_{zz} was recorded at successive fixed ϕ values. The curves are vertically shifted for clarity. (b) $\sigma_{zz}(\theta, \phi)$ at 14 T seen from the $+z$ axis. The dashed circle clearly shows that σ_{zz} is independent of field orientation in the conducting plane except for the narrow angular range around the x axis. (c) Coherence peak at the magnetic field along $\phi = 0$ and $\theta = 90°$.

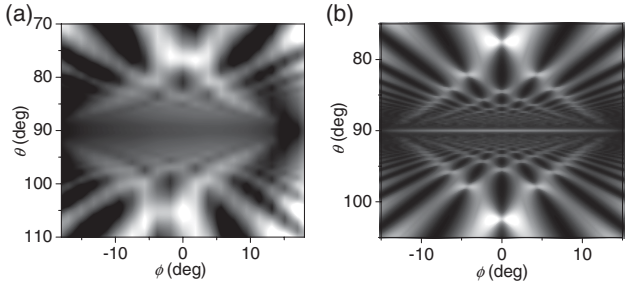

FIG. 3. Density plot of the resistance $R_{zz}(\theta, \phi)$ around the a axis. (a) Experimental data of $R_{zz}(\theta, \phi)$ around the a axis are presented as a density plot in a linear scale. Lighter regions in this plot correspond to larger resistance. The radiating black lines correspond to resistance minima (Lebed resonances). (b) Analytical calculation of $R_{zz}(\theta, \phi)$ around the a axis based on Eq. (2), in a logarithmic scale. The first zeroes of the Bessel functions in the numerator define a well-developed rhombic region and the oscillating nature of the Bessel functions generates the alternating patterns along the radial directions within it. The white horizontal line in (b) represents the coherence peak, also observed experimentally [Fig. 2(c)].

except around the rhombic area; in other words, the shape of the brim forms an almost perfect circle in the xy plane [Fig. 2(b)].

Although most of the observed features are well explained by the models described in Refs. [16,18,20–22], the anomalous conductivity enhancement under in-plane magnetic fields, which appears as the brimlike feature around the xy plane in Fig. 1(a), has not been predicted by any of these models. This feature manifests as a saturating R_{zz} under the magnetic field along the b' direction [13], but the saturation alone is insufficient to explain the insensitivity of σ_{zz} to ϕ over a broad range. The strength of the in-plane anomaly does not scale with B_y, but seems to scale only with B_z and becomes more prominent as the magnetic field increases. Considering that all electron orbits are parallel to the 1D axis and are confined or localized along the stacking direction in the field orientations where the in-plane anomaly appears, the disappearance of the dependence on the in-plane field orientation suggests a decoupling of the 2D conducting layers.

Interlayer decoupling has been discussed in regard to one theoretical model. Strong, Clarke, and Anderson (SCA) proposed a many body theory for the anomalous angular dependence exhibited by $(TMTSF)_2PF_6$ [14,23]. Generally, if a sufficiently strong magnetic field is applied along the y axis, the width of the semiclassical electron orbit can become smaller than the interlayer spacing. SCA conjectured that the electron-electron interaction enhances this confinement effect and decouples the conducting layers into independent 2D non-Fermi liquids. They predicted that the interlayer magnetoresistance in this confinement state scales only with B_z. Qualitatively, this model seems to explain the experimental observation. Quantitatively, however, the experimental interlayer resistance shows B_z-linear scaling rather than the $B_z^{3/2}$ scaling predicted by the SCA theory. Moreover, the region where the B_z-linear scaling occurs is limited by $\tan^{-1}(B_z/B_{\text{plane}}) \lesssim 11.2 \pm 0.7°$ between 1 and 14 T. The fact that this condition is independent of field strength is difficult to explain in terms of the SCA's confinement scenario.

In summary, we have established experimentally the first ever three-dimensional picture of the interlayer conductivity of an anisotropic layered conductor and showed that all the previously reported characteristic oscillatory behaviors in the angular dependence of magnetoresistance are closely related to one another. Either numerical calculation of the interlayer conductivity based on semiclassical electron orbital motion or analytical expressions based on quantum mechanical interlayer tunneling could explain a significant portion of the experimental results, in particular, the Lebed resonances and the modulation of their amplitudes. The Lebed resonance is the only fundamental angular effect, and the other effects result from its amplitude modulation. However, discrepancies were found between existing models and our experimental results, in particular, an anomalous enhancement of the conductivity when the magnetic field lay almost parallel to the conducting plane. The absence of the dependence on in-plane field orientation suggests that interlayer decoupling occurs in the in-plane anomaly. Although the origin of the in-plane anomaly is still unknown, it seems to result from a new electronic state such as a confinement state.

This work was supported by the Korea Science and Engineering Foundation (Grant No. F01-2006-000-10207-0) and by the Korea Research Foundation (Grant No. R14-2003-027-01002-0).

*Author to whom correspondence should be addressed. wkang@ewha.ac.kr

[1] K. Yamaji, J. Phys. Soc. Jpn. **58**, 1520 (1989).
[2] A. G. Lebed, Pis'ma Zh. Eksp. Teor. Fiz. **43**, 137 (1986) [JETP Lett. **43**, 174 (1986)].
[3] M. V. Kartsovnik, Chem. Rev. **104**, 5737 (2004).
[4] T. Osada *et al.*, Phys. Rev. Lett. **66**, 1525 (1991).
[5] M. J. Naughton *et al.*, Phys. Rev. Lett. **67**, 3712 (1991).
[6] W. Kang *et al.*, Phys. Rev. Lett. **69**, 2827 (1992).
[7] H. Kang *et al.*, Phys. Rev. B **68**, 132508 (2003).
[8] G. M. Danner *et al.*, Phys. Rev. Lett. **72**, 3714 (1994).
[9] G. M. Danner *et al.*, Phys. Rev. Lett. **75**, 4690 (1995).
[10] T. Osada *et al.*, Phys. Rev. Lett. **77**, 5261 (1996).
[11] H. Yoshino *et al.*, J. Phys. Soc. Jpn. **68**, 3027 (1999).
[12] I. J. Lee *et al.*, Phys. Rev. B **57**, 7423 (1998).
[13] I. J. Lee *et al.*, Phys. Rev. B **58**, R13343 (1998).
[14] S. P. Strong *et al.*, Phys. Rev. Lett. **73**, 1007 (1994).
[15] A. G. Lebed *et al.*, Phys. Rev. B **55**, R8654 (1997).
[16] R. H. McKenzie *et al.*, Phys. Rev. Lett. **81**, 4492 (1998).
[17] T. Osada, Physica (Amsterdam) **12E**, 272 (2002).
[18] A. G. Lebed *et al.*, Phys. Rev. Lett. **91**, 187003 (2003).
[19] U. Lundin *et al.*, Phys. Rev. B **70**, 235122 (2004).
[20] B. K. Cooper *et al.*, Phys. Rev. Lett. **96**, 037001 (2006).
[21] T. Osada *et al.*, Synth. Met. **103**, 2024 (1999).
[22] P. Moses *et al.*, Phys. Rev. B **60**, 7998 (1999).
[23] D. G. Clarke *et al.*, Science **279**, 2071 (1998).
[24] T. Osada, Physica (Amsterdam) **256–258B**, 633 (1998).
[25] T. Osada *et al.*, Physica (Amsterdam) **18E**, 200 (2003).
[26] T. Osada *et al.*, Synth. Met. **135–136**, 653 (2003).
[27] A. G. Lebed *et al.*, Phys. Rev. Lett. **93**, 157006 (2004).
[28] A. G. Lebed *et al.*, Phys. Rev. B **71**, 132504 (2005).
[29] The brimlike feature is universal in the $(TMTSF)_2X$ salts. Two other compounds, $X = ClO_4$ (1 bar) and ReO_4 (10.8 kbar), showed the similar feature.